

An Extension of the Hammond Postulate. Structural Effects on the Classification of Chemical Reactions

Felipe A. Bulat and Alejandro Toro-Labbé*

Laboratorio de Química Teórica Computacional (QTC), Facultad de Química, Pontificia Universidad Católica de Chile, Casilla 306, Correo 22, Santiago, Chile

Received: September 9, 2002

Combination of the reaction energy, a thermodynamic index, with structural descriptors, such as the force constants associated with the reactant and products potential wells, allows us to define a new index that quantifies the position of the transition state and classifies reactions in terms of their Hammond or anti-Hammond character. Switching from the classical restricted Hammond behavior to a general behavior, in which the position of the transition state is not only conditioned by energy comparisons, occurs through adding a new term accounting for the structural effects in the potential-energy function. It is shown that these effects strongly influence the position of transition states but leave the barrier height practically unchanged. Analysis of 27 chemical reactions of different types, such as rotational isomerizations, SN2, and intramolecular reordering reactions, provides strong support to the model presented here.

1. Introduction

The Hammond postulate (HP)¹ is a central concept in physical chemistry because of the constraints it establishes on the position of a transition structure in terms of the energies of reactants and products. Indeed, the HP asserts that the transition state (TS) on a single-step reaction will be located nearer the stationary state with the higher energy content. In other words, exothermic reactions will have an *early* barrier, while endothermic reactions are supposed to present *late* barriers. Although its qualitative nature is evident, the HP has been invoked extensively as a tool to get insights about the structure of the TS from the knowledge of reactants and products. A word of caution is to be considered here;² the HP, as originally stated, does not necessarily hold when the activation energy is big compared to the reaction energy.

Various formulations and variations of the HP have been proposed over the years, and there exist several principles and theories that may be regarded as quantitative formulations of it (see ref 3 and references therein). Among them, the Leffler postulate⁴ has been named by Murdoch⁵ an “extended Hammond Postulate”. Leffler’s postulate asserts that the partial derivative of the energy barrier with respect to the reaction energy equals the position of the TS, that along a reduced reaction coordinate defines the Brønsted coefficient. It is worth mentioning a very successful approach by Miller⁶ that leads to an expression for the position of the TS that is independent of the functional form of the reaction coordinate. Agmon³ recovered Miller’s expression using the bond order as a reaction coordinate for simple $A + BC \rightarrow AB + C$ reactions. To the best of our knowledge, Miller’s expression seems to be the most successful approach in quantifying the HP from a purely *classical* point of view.

Among more recent approaches, it is worth mentioning the use of similarity indexes to quantify the vague notion of *late* and *early* TS. Within these, Cioslowski⁷ proposed a similarity index based on the reduced first-order density matrices that accounts for the structural distance between two species.

Although structural distance is in itself a slippery concept, it has been widely used within different existing approaches.⁸

Because structural distance is not uniquely defined, it cannot give exact accounting for the HP. Furthermore, the nonuniqueness of the structural distance definition allows dramatic changes in the relative location of a TS with respect to reactants and products, and hence, stating that a particular process “violates the Hammond postulate” is dangerous because the very same process that violates it under a given definition of the structural distance may perfectly hold under another one. Arteca and Mezey⁹ stated, while studying molecular shapes and its changes along reaction paths, that “the reinterpretation of the Hammond Postulate according to similarity defined by shape descriptors may reclassify some reactions, showing a formal violation according to the standard formulation”. The bottom line of this line of argument is that we must accept that while the HP seems to hold on a particular framework, it may fail according to another one. One way around it would be to accept a particular choice of similarity and provide a model flexible enough to accurately account for the cases that follow the HP, as well as for those that do not.

In this article, expressions that quantify what we call extended Hammond postulate (EHP) through the position of the transition state are proposed. Within this model, Hammond as well as anti-Hammond processes are accounted for; both behaviors can be rationalized through the topological properties of the potential energy surface in the directions that lead to the transition structure in the N -dimensional configurational space.

It is widely accepted that the force constants associated with the reactants and product potential energy wells are responsible for the anti-Hammond behavior.^{10,11} Indeed, small changes in the force constants may modify the topology of the energy profile along the reaction coordinate enough to overcome the tendency imposed by thermodynamics through the Hammond postulate. The explicit consideration of force constants of reactants and products is what makes our model flexible enough to account for the EHP. While the HP is based on the reaction

* To whom correspondence should be addressed. E-mail: atola@puc.cl.

energetics only, the EHP also considers the force constants associated with the reactant and product potential wells.

The EHP herein outlined attempts to classify reactions as Hammond or anti-Hammond through qualitative and quantitative descriptors readily available from the present analysis. A generalized, quantitative version of the Hammond postulate should be applicable to every kind of process. Indeed, our approach is applicable even in cases in which the reaction energy is rather small when compared to the activation energy, one of the most important drawbacks of the original postulate.²

This article is organized as follows. After succinctly introducing the reader to the model potential used throughout the article, the general results leading to a flexible description of the reaction profile are presented. During such analysis, we introduce indexes capable of classifying and quantifying the EHP through the position of the transition structure. In section 3, the theoretical models used in the calculations and parameters necessary for analyzing different chemical processes are discussed. Section 4 presents applications of the EHP to rotational isomerizations and other chemically interesting processes. Section 5 contains our concluding remarks.

2. Theoretical Model

2.1. Torsional Potential. In previous articles,^{12–15} the usage of symmetry-adapted limited Fourier series (LFS) expansions as an appealing choice for describing rotational isomerization processes was discussed. Such conformational functions along a torsional angle α were conveniently expressed as follows:

$$V(\alpha) = V_0(\alpha) + V_1(\alpha) \quad (1)$$

$$V_0(\alpha) = \frac{1}{2}\Delta V^0(1 - \cos \alpha) + \frac{1}{4}(k_R + k_P)(1 - \cos^2 \alpha) \quad (2)$$

$$V_1(\alpha) = \frac{1}{4}(k_R - k_P - \Delta V^0)(1 - \cos^2 \alpha)\cos \alpha \quad (3)$$

where $\Delta V^0 = V(\alpha_P) - V(\alpha_R)$ is the reaction energy and k_P and k_R are the force constants associated with the reactant (R) and product (P) potential wells.

It is useful to define the reduced reaction coordinate (RRC), ω , which for the case of rotational isomerizations can be expressed as follows:¹⁵

$$\omega(\alpha) = \frac{1}{2}(1 - \cos \alpha) \quad \omega \in [0, 1] \quad (4)$$

Applying the inverse transformation to eq 1, we obtain

$$V[\omega] = V_0[\omega] + V_1[\omega] \quad (5)$$

$$V_0[\omega] = \Delta V^0\omega + K_V\omega(1 - \omega) \quad K_V = k_P + k_R \quad (6)$$

$$V_1[\omega] = (\Delta k^0 + \Delta V^0)\omega(1 - \omega)(2\omega - 1) \quad \Delta k^0 = k_P - k_R \quad (7)$$

It is interesting to note that eq 5 can be regarded as a general potential function describing the energy evolution along a RRC for a general single-barrier process. Only when ω is given by eq 4, the symmetry-adapted LFS expansion for the torsional potential arises. Hence, eq 5 is a general potential that for particular choices of the RRC takes the appropriate form for that particular problem. Moreover, $V_0[\omega]$ has been successfully used for the rationalization of various chemical processes, although

the explicit RRCs were not known in most cases.¹⁶ Indeed, we have previously described an approach,^{15–17} based on the potential $V_0[\omega]$, for quantifying the Brønsted coefficient, β , a parameter that gives the position of the TS along the reaction coordinate:

$$\left. \frac{dV_0[\omega]}{d\omega} \right|_{\omega=\beta} = 0 \Rightarrow \beta = \frac{1}{2} + \frac{\Delta V^0}{2K_V} \quad (8)$$

where β quantifies the HP because any shift from the value 0.5 depends only on the sign of ΔV^0 , that is, for exothermic reactions $\Delta V^0 < 0$ leads to $\beta < 1/2$ while for endothermic reactions $\Delta V^0 > 0$ implies $\beta > 1/2$, in consistency with what is expected from the HP.

$V_0[\omega]$ is also consistent with the Leffler's postulate, which ensures that the derivative of the activation energy ΔV^\ddagger with respect of the overall energy change ΔV^0 equals the position of the transition state:⁴

$$\frac{\partial \Delta V^\ddagger}{\partial \Delta V^0} = \beta = \frac{1}{2} + \frac{\Delta V^0}{2K_V} \quad (9)$$

Replacing the expression for β in $V_0[\omega]$, we obtain an expression that quantifies the energy barrier, ΔV^\ddagger , that is consistent with the Hammond and Leffler postulates:

$$V_0[\beta] \equiv \Delta V^\ddagger = \frac{1}{4}K_V + \frac{\Delta V^0}{2} + \frac{(\Delta V^0)^2}{4K_V} \quad (10)$$

This expression is the Marcus equation.¹⁸ It must be stressed that all of these quantities depend only upon two parameters, K_V and ΔV^0 , so the above formulas provide useful and rather simple tools for characterizing the transition state of Hammond processes.^{15–17}

2.2. Characterization of Hammond and anti-Hammond Processes. Let us go further and use the whole potential function (eq 5) to define the coefficient γ through the first derivative of eq 5 evaluated at $\omega = 0.5$, the midpoint between reactants and products:

$$\left. \frac{dV[\omega]}{d\omega} \right|_{\omega=0.5} = \frac{1}{2}(3\Delta V^0 + \Delta k^0) = \gamma \quad (11)$$

Note that γ can be seen as a structural and thermodynamic index because it includes the overall change of both the force constants through $\Delta k^0 = k_P - k_R$ and the total energy through ΔV^0 . Evidently, the sign of γ indicates whether the TS is located nearer the products (positive γ) or nearer the reactants (negative γ). Then, for the case of endothermic processes ($\Delta V^0 > 0$), we have (see Figure 1a)

$$\gamma > 0 \Rightarrow \beta_0 > 0.5 \quad (\text{Hammond process})$$

$$\gamma < 0 \Rightarrow \beta_0 < 0.5 \quad (\text{anti-Hammond process})$$

where β_0 stands for the actual position of the TS of the reaction. For exothermic processes ($\Delta V^0 < 0$), it can be similarly stated that (Figure 1b)

$$\gamma < 0 \Rightarrow \beta_0 < 0.5 \quad (\text{Hammond process})$$

$$\gamma > 0 \Rightarrow \beta_0 > 0.5 \quad (\text{anti-Hammond process})$$

Note that the signs of γ and ΔV^0 are the same for Hammond cases while they are opposite for anti-Hammond ones; therefore,

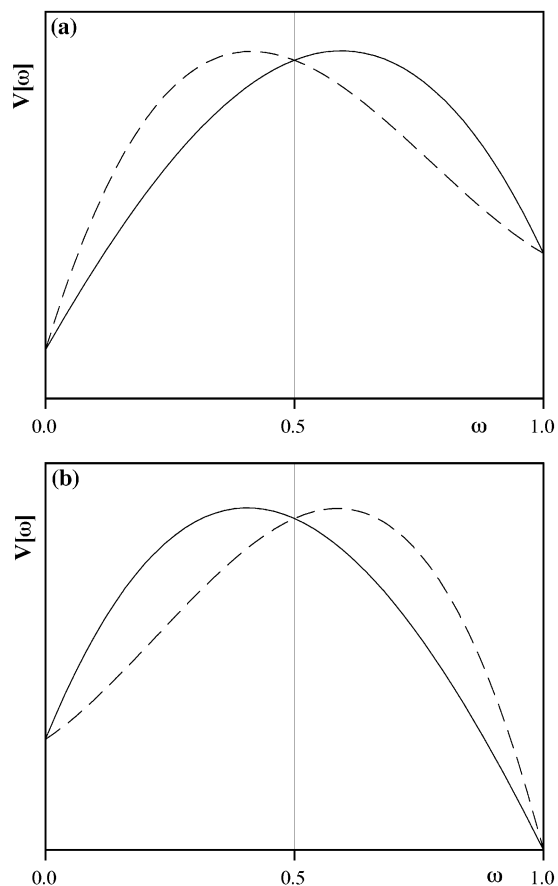


Figure 1. Sketch of (a) endothermic and (b) exothermic (—) Hammond and (---) anti-Hammond processes.

one can safely claim that for Hammond processes

$$\frac{\gamma}{\Delta V^0} = \frac{3\Delta V^0 + \Delta k^0}{2\Delta V^0} > 0$$

while for anti-Hammond processes

$$\frac{\gamma}{\Delta V^0} = \frac{3\Delta V^0 + \Delta k^0}{2\Delta V^0} < 0$$

a result that is summarized as follows:

$\gamma/\Delta V^0$	$\gamma > 0$	$\gamma < 0$
$\Delta V^0 > 0$	Hammond	anti-Hammond
$\Delta V^0 < 0$	anti-Hammond	Hammond

Note that also when $\gamma = 0$ and then $\gamma/\Delta V^0 = 0$ the reaction is always anti-Hammond unless $\Delta V^0 = 0$ and $k_R = k_P$ because symmetric reactions lie within the Hammond type of reactions, as confirmed by eq 9. In such a case, the index $\gamma/\Delta V^0$ is not defined.

It is quite clear by now that what corrects the rigidity of the potential $V_0[\omega]$ is the explicit consideration of an additional degree of freedom, namely, Δk^0 , through the inclusion of $V_1[\omega]$. Figure 2a) shows the effect of such a parameter by plotting the family of curves spanned by a fixed set of $\{\Delta V^0, K_V\}$ (arbitrarily taken as $\Delta V^0 = 1$ and $K_V = 10$) values while allowing Δk^0 to vary from $-0.8K_V$ to $0.8K_V$ in a $0.2K_V$ step thus obtaining $\Delta k^0 = -8, -6, \dots, 0, \dots, 6, 8$. Note in Figure 2 the case $\Delta k^0 = -\Delta V^0$ (thick line) in which $V[\omega] = V_0[\omega]$

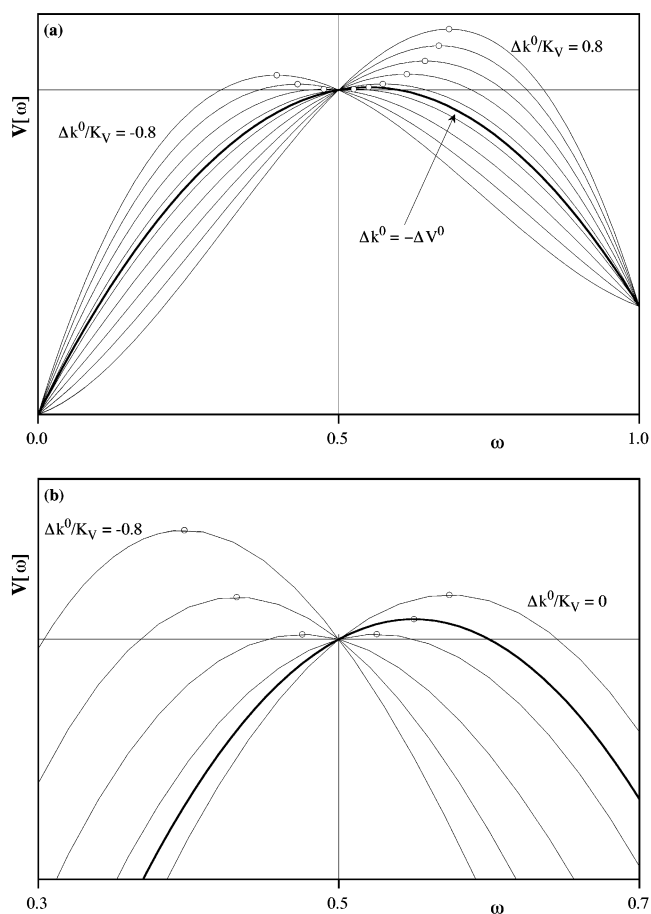


Figure 2. Curve family (a) spanned by fixed $\{\Delta V^0, K_V\}$ and $-0.8K_V \leq \Delta k^0 \leq 0.8K_V$. $V_0[\omega]$ at $\{\Delta V^0, K_V\}$ is shown by the thick line. The circles show the position of the TS. The horizontal gray line is located at $V[0.5] = V_0[0.5] + \Delta V^0/2$. Panel b shows a close up of the TS region of panel a narrowing the range of Δk^0 within the interval $-0.8K_V \leq \Delta k^0 \leq 0$.

because $\Delta V^0 + \Delta k^0 = 0$ and then $V_1[\omega] = 0$. Note that according to the Δk^0 value (for a given $\{\Delta V^0, K_V\}$) a particular process might present either a *late* or an *early* TS.

It is also worth noting that the value of the potential at $\omega = 0.5$ is independent from Δk^0 , which turns out to be quite obvious because $V_1[0.5] = 0$ ($V[0.5] = V_0[0.5] = 1/4K_V + 1/2\Delta V^0$). So far, the point $\omega = 0.5$ presents two remarkable properties, namely, a derivative that qualitatively classifies a given process through the γ index and a value for the potential that is independent of Δk^0 .

Another conclusion drawn from Figure 2 is that while Δk^0 strongly influences the TS position, it has little effect on the barrier height. Indeed, taking $V_0[\omega]$ as reference (thick line, with the TS at $\beta = 0.55$), as shown in Figure 2a, a $-0.8K_V$ value for Δk^0 locates the TS position at 0.39 (roughly 30% from the reference value of 0.55), while the change in the barrier height amounts roughly to 4%. On the other hand, using $\Delta k^0 = 0.8K_V$, we obtain the position of the TS at 0.68 (roughly a 24% change) and the change in ΔV^\ddagger goes up to 17%. It must be stressed that such variations are limiting cases and in practice the $\Delta k^0/K_V$ values are negative for endothermic cases and positive for exothermic reactions because for *deeper* potential wells force constants are expected to be quite high. In fact, we could further constrain the Δk^0 values to the interval $[-K_V, 0]$ for $\Delta V^0 > 0$ reactions while to $[0, K_V]$ for $\Delta V^0 < 0$ cases because

$$\Delta V^0 > 0 \rightarrow k_p \leq k_R \rightarrow \Delta k^0 < 0$$

$$\Delta V^0 < 0 \rightarrow k_p \geq k_R \rightarrow \Delta k^0 > 0$$

Hence, as seen in Figure 2b ($\Delta k^0 \in [-K_V, 0]$, $\Delta V^0 > 0$), we should expect small variations for the barrier heights (less than 4%). It should be stressed that such variations on Δk^0 tend, in general, to shift the TS position toward the anti-Hammond behaviors.

2.3. The Brønsted Coefficient. In the previous section, interesting information concerning the type of process was obtained with the sole usage of three parameters (k_R , k_P , and ΔV^0). Now, an expression for the Brønsted coefficient by maximizing $V[\omega]$ can be obtained:

$$\left. \frac{dV[\omega]}{d\omega} \right|_{\omega=\beta'} = 0$$

Note that $\beta' \neq \beta$ because β was obtained from $V_0[\omega]$. Solving for β' and choosing the correct solution of the quadratic equation, we obtain the following expression accounting for the position of the TS:

$$\beta' = \frac{1}{2} + \frac{\sqrt{6(\Delta V^0 + \Delta k^0)\gamma + K_V^2} - K_V}{6(\Delta V^0 + \Delta k^0)} \quad (12)$$

The fact that β' is a maximum is ensured because the second derivative of $V[\omega]$ at β' is given by $-2\sqrt{3(\Delta V^0 + \Delta k^0)\gamma + K_V^2}$, and hence, for real values of β' , it necessarily corresponds to a maximum. In the present framework, an analytic expression for ΔV^\ddagger presents no practical interest because of the complicated expression that is encountered by putting β' into $V[\omega]$. Nevertheless, the numerical values of β' can be introduced in eq 5 providing values for the energy barrier (ΔV^\ddagger) that are comparable to those obtained through the use of eq 10.

In a recent article,¹⁹ it has been shown that a good approximation to β' can be obtained through the use of bifurcation theory (BT); this leads to

$$\beta' \approx \beta_{BT} = \frac{1}{2} + \frac{3\Delta V^0 + \Delta k^0}{4K_V} = \frac{1}{2} + \frac{\gamma}{2K_V} \quad (13)$$

This is a very important result because it shows a linear relationship between the position of the TS and γ/K_V , which suggests that the γ coefficient may be used not only to classify but also to quantify the EHP through the position of the TS. Even more, by substituting β_{BT} into $V[\omega]$, one obtains an expression for the energy barrier (ΔV_{BT}^\ddagger), which can be conveniently expressed in terms of the Marcus equation (ΔV^\ddagger):

$$V(\beta_{BT}) \equiv \Delta V_{BT}^\ddagger = \Delta V^\ddagger + \frac{(\Delta k^0 + \Delta V^0)}{4K_V} \left(\frac{\Delta k^0 + 5\Delta V^0}{4} - \frac{\gamma^3}{K_V^2} \right) \quad (14)$$

Note that these expressions, eqs 13 and 14, are consistent with the $V[\omega]$ separation into $V_0[\omega]$ and $V_1[\omega]$, that is, when $\Delta k^0 + \Delta V^0 = 0$ then $V[\omega] = V_0[\omega]$ and the Marcus equation is recovered from eq 14 while β is recovered from eq 13. The expression for β_{BT} in terms of β ,

$$\beta_{BT} = \frac{1}{2} + \frac{\Delta V^0}{2K_V} + \frac{\Delta V^0 + \Delta k^0}{4K_V} = \beta + \frac{\Delta V^0 + \Delta k^0}{4K_V} \quad (15)$$

is seen as a correction to β by the term $(\Delta V^0 + \Delta k^0)/(4K_V)$, which may become quite important, while the perturbation to the Marcus equation shown in eq 14 is quite small. Hence, within this new framework, the Marcus equation continues to be reliable.

It is interesting to note the similar structure that both the HP- and EHP-consistent indexes (β and β_{BT}) present:

$$\frac{1}{2} + \frac{1}{2K_V} \left(\frac{df[\omega]}{d\omega} \right)_{\omega=0.5}$$

where $f[\omega]$ corresponds to either $V_0[\omega]$ or $V[\omega]$. When using $V_0[\omega]$, the above expression leads to β (eq 9); the thermodynamic index ΔV^0 in eq 9 is replaced by a combined structural–thermodynamic index γ when the complete potential function $V[\omega]$ is used instead, thus switching from the HP to the EHP behaviors.

2.4. Extension to Nonrotational Systems. So far, strictly speaking, all of these results are mainly applicable to rotational systems, for which the potential was originally proposed.¹² Nevertheless, as stated in section 2.1, the expression for $V[\omega]$ can be seen as a generalized potential function in a RRC, which takes specific functional forms when specific RRCs are used, as is the case for rotational isomerizations. The main difficulty in applying our results to nonrotational processes is the calculation of force constants for reactants and products. While for rotational isomerization a simple formula is readily available,¹⁵ for other kinds of reactions the scheme is more complicated. Evidently, it would be desirable to be able to use ab initio or experimental force constants.

Evidently, when one uses the Marcus equation to estimate K_V , from the knowledge of the reaction and activation energies, the coordinate system is the generalized RRC ω . If we were able to determine the individual force constants (or just Δk^0) in the same coordinate system, we would avoid the need for explicit expression for the RRC, as eq 4 for the rotational cases; this is not a simple task. Fortunately, this situation can be circumvented when noting that Δk^0 can be expressed as follows:

$$\Delta k^0 = K_V \left(\frac{C_k - 1}{C_k + 1} \right) \quad C_k = \frac{k_P}{k_R} \quad (16)$$

This expression for Δk^0 is quite convenient because the value obtained for it is consistent with the coordinate system for the K_V value (for example, arising from the Marcus equation).

Murdoch,⁵ when analyzing the conditions leading to Miller's expression for the TS position,⁶ stated that "Theoretically, it is quite mysterious why the barrier position should be independent of the specific functional form of the reaction coordinate and should depend only on the barrier height and the reaction thermodynamics". This is precisely what happens also with Marcus equation, and hence, the use of it for the estimation of K_V and Δk^0 through eq 16 makes it *independent* of the reaction coordinate. This fact reinforces the relation of β_{BT} with empirical indexes such as the Brønsted coefficient. This is truly the case because our proposal is to treat β_{BT} as a correction to β arising from $V_0[\omega]$.

Using eq 16, we may rewrite β_{BT} as

$$\beta_{BT} = \beta + \frac{\Delta V^0}{4K_V} + \frac{1}{4} \left(\frac{C_k - 1}{C_k + 1} \right) \quad (17)$$

which is the expression used in the estimation of the TS position

TABLE 1: Studied Processes and Model Chemistries

number	reactant	product	method	refs
R1	<i>t</i> -HSNS	<i>c</i> -HSNS	HF/6-31G(d,p)	15
R2	<i>t</i> -FSNO	<i>c</i> -FSNO	HF/6-31G(d,p)	15
R3	<i>t</i> -CHO-CHO	<i>c</i> -CHO-CHO	HF/6-31G(d,p)	15
R4	<i>t</i> -CFO-CHO	<i>c</i> -CFO-CHO	HF/6-31G(d,p)	15
R5	<i>t</i> -CCIO-CHO	<i>c</i> -CCIO-CHO	HF/6-31G(d,p)	15
R6	<i>t</i> -CHO-CHO	<i>c</i> -CHO-CHO	HF/6-311G(d,p)	21
R7	<i>t</i> -CFO-CHO	<i>c</i> -CFO-CHO	HF/6-311G(d,p)	21
R8	<i>t</i> -CCIO-CHO	<i>c</i> -CCIO-CHO	HF/6-311G(d,p)	21
R9	<i>t</i> -CHO-CHO	<i>c</i> -CHO-CHO	HF/6-311++G	21
R10	<i>t</i> -CFO-CHO	<i>c</i> -CFO-CHO	HF/6-311++G	21
R11	<i>t</i> -CCIO-CHO	<i>c</i> -CCIO-CHO	HF/6-311++G	21
R12	<i>t</i> -CHO-CHO	<i>c</i> -CHO-CHO	HF/6-311++G(d,p)	21
R13	<i>t</i> -CFO-CHO	<i>c</i> -CFO-CHO	HF/6-311++G(d,p)	21
R14	<i>t</i> -CCIO-CHO	<i>c</i> -CCIO-CHO	HF/6-311++G(d,p)	21
R15	<i>t</i> -CHO-CHO	<i>c</i> -CHO-CHO	B3LYP/6-311++G(d,p)	21
R16	<i>t</i> -CFO-CHO	<i>c</i> -CFO-CHO	B3LYP/6-311++G(d,p)	21
R17	<i>t</i> -CCIO-CHO	<i>c</i> -CCIO-CHO	B3LYP/6-311++G(d,p)	21
R18	Cl ⁻ + CH ₃ F	CICH ₃ + F ⁻	B3LYP/6-311++G(df,pd)	22
R19	H ₂ CC:	HCCH	CCSD/6-311G(d,p)	23
R20	HONS	HSNO	HF/6-31G(d)	24
R21	H ₂ SO	HSOH	HF/6-31G(d)	24
R22	<i>t</i> -HOC=SH	<i>c</i> -HOC=SH	HF/6-311G(d,p)	12
R23	<i>t</i> -HOC=SH	<i>c</i> -HOC=SH	B3LYP/6-311G(d,p)	12
R24	<i>t</i> -HOC=SH	<i>t</i> -HO=CSH	HF/6-311G(d,p)	25
R25	<i>t</i> -HOC=SH	<i>t</i> -HO=CSH	B3LYP/6-311G(d,p)	25
R26	<i>t</i> -HO=CSH	<i>c</i> -HO=CSH	HF/6-311G(d,p)	12
R27	<i>t</i> -HO=CSH	<i>c</i> -HO=CSH	B3LYP/6-311G(d,p)	12

for nonrotational systems with K_V coming from the Marcus equation and Δk^0 from eq 16.

3. Computational Methods

Different model chemistries were used to address different kinds of problems throughout this article. Indeed, because very different processes are herein studied, the theoretical methods range from Hartree-Fock to coupled-cluster techniques. Table 1 shows the different reactions studied, the level of calculations employed to address each of them, and the corresponding references on each subject. Figure 3 sketches the different kinds of processes studied. For all calculations, we have used the Gaussian 98 package²⁰ to perform full geometry optimizations at each stationary state of all systems; frequency calculations indicated whether they correspond to local minima or first-order saddle points.

The force constants ($k_{R=trans}$ and $k_{P=cis}$) for rotational isomerizations were obtained through the following expression, which required additional points on the PES:¹²⁻¹⁵

$$k_{R/P} = - \sum_{n=1}^{N_p} \sum_{i=1}^{N_p} n^2 C_{i,n} \cos(n\alpha_{R/P}) V(\alpha_i) \quad (18)$$

where N_p is the number of computed energy points used to fit local potential wells at R and P, $V(\alpha_i)$ is the energy at the point α_i and $C_{i,n}$ are the elements of the inverse matrix $[\cos(i\alpha_n)]^{-1}$. It has been shown that the $k_{R/P}$ values are, to a good approximation, independent of N_p and using $N_p = 2$ leads to quite good results out of few energy points. Considering that the trans isomer is defined to be at $\alpha = 0^\circ$ and hence the cis isomer to be at $\alpha = 180^\circ$, $k_R = k_t$ can be determined from the energy points $\alpha_1 = 0^\circ$ and $\alpha_2 = 10^\circ$, while $k_P = k_c$ can be estimated from the energy points $\alpha_1 = 170^\circ$ and $\alpha_2 = 180^\circ$.¹⁵

Through k_t and k_c , the parameters K_V and Δk^0 are readily estimated, and hence, γ , β , β' , and β_{BT} can be estimated through eqs 11, 8, 12, and 13, given the reaction energy ΔV^0 from the ab initio calculations. The energy barrier may be estimated from eqs 10 and 14. Alternatively, K_V may be estimated from eq 10

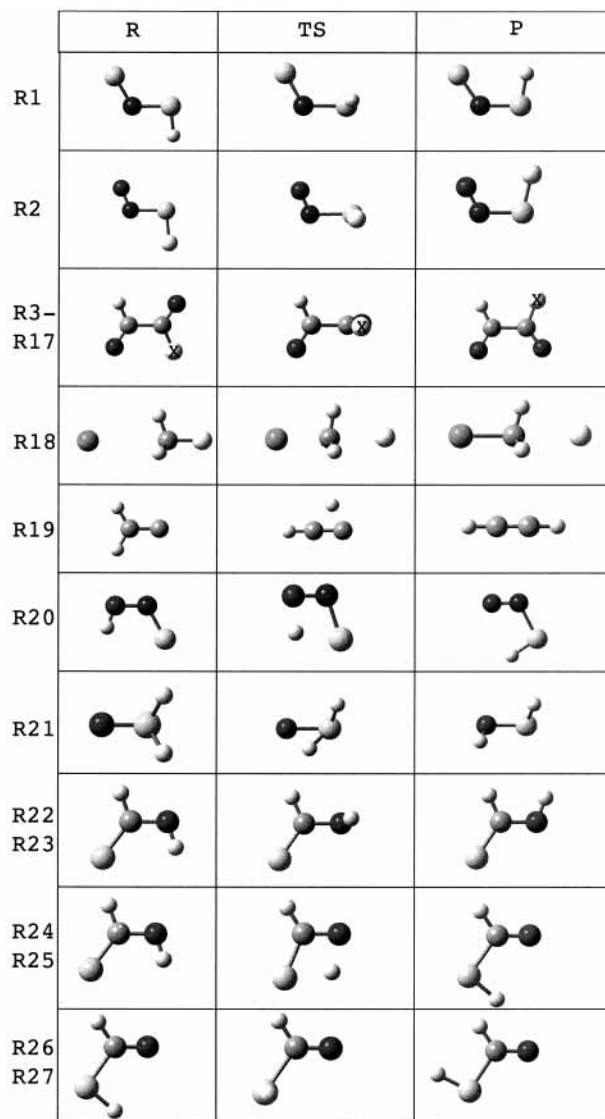


Figure 3. Reactions considered in the present study. For R3–R17, when X = H the reactions are R3, R6, R9, R12, and R15, when X = F the reactions are R4, R7, R10, R13, and R16, and when X = Cl the reactions are R5, R8, R10, R14, and R17.

if ΔV^\ddagger is known from the ab initio calculations. In such a case, Δk^0 may be estimated through eq 16 with the dimensionless ratio $C_k = k_P/k_R$ estimated from ab initio frequency calculations at R and P. Consequently, the values for γ , β , β' , and β_{BT} can be reevaluated. These two methodologies are used throughout the numerical estimations when appropriate.

Reactions R1–R17 correspond to rotational isomerizations. The data for R1–R5 has been taken from previous studies¹⁵ in which the force constants, k_R and k_P , have been estimated using eq 18. The force constants for reactions R6–R17 have been determined by both eq 18 and the ab initio calculations. The remaining reactions, that is, R18–R27, correspond to SN2 reactions (R18), intramolecular proton transfers (R19–R21, R24, and R25), and rotational isomerizations (R22, R23, R26, and R27). For all of these reactions, the force constants have been estimated from ab initio frequency calculations.

While for rotational isomerizations the RRC is explicitly defined and depends only on the dihedral angle, its optimized value at the TS may be used in eq 4 to estimate the actual position of the TS along the RRC, β_0 . The estimated values for the Brønsted coefficient must be compared with the reference β_0 value. As for nonrotational processes, there is no RRC

TABLE 2: Calculated and Estimated Energy Barriers, TS Positions, and Type Assignment According to $\gamma/\Delta V^0$ ^a

system	ΔV_0^\ddagger	ΔV^\ddagger	$\Delta V_{\text{BT}}^\ddagger$	β_0	γ	$\gamma/\Delta V^0$	type
R1	12.63	13.38	13.38	0.53	0.69	-4.60	aH
R2	12.76	13.89	13.87	0.52	0.81	-0.36	aH
R3	7.81	7.22	7.04	0.60	4.50	0.79	H
R4	5.29	4.45	4.44	0.50	0.03	0.03	H
R5	5.33	4.80	4.71	0.52	0.75	0.31	H
R6	6.84	6.18	6.16	0.58	5.34	0.98	H
R7	4.55	3.88	3.86	0.51	1.51	0.86	H
R8	4.09	3.60	3.52	0.50	1.28	0.58	H
R9	6.83	6.40	6.20	0.57	4.54	0.81	H
R10	4.17	3.29	3.28	0.48	-0.19	-0.25	aH
R11	3.79	3.22	3.12	0.49	-0.17	-0.09	aH
R12	6.41	5.89	5.84	0.65	5.34	0.95	H
R13	4.12	3.41	3.37	0.52	1.41	0.75	H
R14	3.36	2.74	2.62	0.50	0.91	0.45	H
R15	5.95	4.93	4.97	0.61	4.72	1.05	H
R16	3.19	2.43	2.44	0.52	1.16	1.13	H
R17	2.58	1.91	1.86	0.47	-0.13	-0.13	aH

^a Energies in kcal mol⁻¹.

expression; hence, β_0 is not defined, and our reference will be defined in terms of the following structural distance:

$$d(A,B) = \sum_i^N \sum_{j<i}^N (\mathcal{D}_{ij}^A - \mathcal{D}_{ij}^B)^2 \quad (19)$$

where \mathcal{D}_{ij}^X are the elements of the distance matrix for structure X and N is the number of atoms in X . Because the distance matrix has $N(N-1)/2$ distinct elements and any N -nuclei structure has $3N-6$ degrees of freedom, it is evident that the distance matrix completely specifies a rigid body because $N(N-1)/2 \geq 3N-6$ for all $N \geq 3$ (in fact, when $N > 4$, it specifies an overrigid body). This definition can be shown to correspond to a metric of a $3N-6$ configurational space. The measure of the relative distance from reactants to TS,

$$\tau = \frac{d(R,TS)}{d(R,TS) + d(TS,P)} \quad 0 < \tau < 1 \quad (20)$$

should be comparable to the Brønsted coefficient. Although τ does not correspond to the *advancement of the reaction* at the TS because this later should be related to the length of the reaction path, it should in general provide a reference for the relative TS position.

4. Results and Discussion

4.1. Rotational Isomerization Reactions: R1–R17. *The Barrier Height and the HP Behavior.* It was stated in section 2.2 that the barrier height should not be affected by the correction $V_1[\omega]$ to the model potential $V_0[\omega]$ (see Figure 2). Table 2 shows the calculated (ΔV_0^\ddagger) and estimated energy barriers (through both eqs 10 and 14, entries ΔV^\ddagger and $\Delta V_{\text{BT}}^\ddagger$, respectively). It is quite obvious that the term that is summed up to the Marcus equation to yield $\Delta V_{\text{BT}}^\ddagger$ (eq 14) is fairly small because practically there is no variation from the ΔV^\ddagger values. This result confirms the statement of section 2.3 suggesting that unlike the TS position the height of the barrier is not affected by structural parameters such as Δk^0 .

While the Hammond or anti-Hammond character of a given process may be determined by observing the TS position along the RRC and the sign of ΔV^0 , the newly proposed coefficients γ and $\gamma/\Delta V^0$ provide a precise characterization of the processes in terms of the HP. Table 2 also shows β_0 (the *actual* location of the TS), γ , and $\gamma/\Delta V^0$ indexes (force constants through eq

TABLE 3: Calculated and Estimated TS Positions (Brønsted Coefficients) and Type Assignments According to β_0 ^a

system	ΔV^0	k_R	k_P	β_0	β	β'	β_{BT}	type
R1	-0.15	26.00	27.83	0.53	0.50	0.51	0.51	aH
R2	-2.21	25.83	34.07	0.52	0.48	0.51	0.51	aH
R3	5.69	11.74	3.66	0.60	0.68	0.66	0.65	H
R4	0.80	9.25	6.90	0.50	0.52	0.50	0.50	aH
R5	2.43	9.86	4.06	0.52	0.59	0.53	0.53	H
R6	5.44	8.43	2.78	0.58	0.74	0.74	0.74 (0.63)	H
R7	1.76	7.00	4.73	0.51	0.58	0.57	0.56 (0.52)	H
R8	2.19	6.77	2.76	0.50	0.62	0.57	0.57 (0.50)	aH
R9	5.60	9.72	1.99	0.57	0.74	0.72	0.69 (0.62)	H
R10	0.77	7.11	4.42	0.48	0.54	0.49	0.49 (0.48)	aH
R11	1.88	7.33	1.36	0.49	0.61	0.49	0.49 (0.44)	aH
R12	5.63	7.44	1.22	0.65	0.83	0.83	0.83 (0.67)	H
R13	1.87	6.15	3.36	0.52	0.60	0.58	0.57 (0.52)	H
R14	2.01	5.26	1.05	0.50	0.66	0.58	0.57 (0.48)	aH
R15	4.48	6.16	2.15	0.62	0.77	0.77	0.78 (0.61)	H
R16	1.03	4.14	3.37	0.52	0.57	0.58	0.58 (0.51)	H
R17	0.96	4.33	1.20	0.47	0.59	0.49	0.49 (0.42)	aH

^a Energies in kcal mol⁻¹; force constants in kcal mol⁻¹ rad⁻².

18, shown in Table 3). Except for R1 and R2, all reactions are endothermic, $\Delta V^0 > 0$ (see Table 3); accordingly, through the HP, we should expect the TS for R1 and R2 to be *early* and those for R3–R17 to be *late*. We see that this is not the case for reactions R1 and R2 with $\beta_0 > 0.50$ and R10, R11, and R17 with $\beta_0 < 0.50$. Note that the $\gamma/\Delta V^0$ index successfully identifies those reactions as anti-Hammond processes (see the type entry); this confirms the reliability of $\gamma/\Delta V^0$ as a qualitative index.

Note that, strictly speaking, reactions R4, R8, and R14, for which the TS is located midway between reactants and products (with $\Delta V^0 \neq 0$), correspond also to anti-Hammond behaviors; our $\gamma/\Delta V^0$ index fails in assigning the right behavior to these reactions. Evidently, when the TS is close to $\beta = 0.5$, the γ index should be close to zero (see the γ value for R4). Hence, small numerical error in the estimation of the force constants may easily shift γ from a negative to a positive value or vice versa. Although the γ value for R4 is small, indicating a TS around 0.5, it is not the case for R8 and R14. Nevertheless, if the ab initio force constants are used to estimate γ , the $\gamma/\Delta V^0$ values for R8 and R14 are reevaluated to 0.02 and -0.21. This better qualitative classification is clearly a consequence of the more accurate γ index, which provides a better agreement with the β_0 , as seen in Table 3.

The Brønsted Coefficient. Table 3 shows the reaction energy, the force constants (through eq 18), β_0 , and the Brønsted coefficients from eqs 8, 12, and 13, β , β' , and β_{BT} , respectively. The value in parentheses under the β_{BT} entry is estimated from the ab initio force constants (not shown).

As seen from Table 3, the β coefficient, which follows from a HP-consistent potential function, assigns *late* or *early* barriers to all processes according to Hammond's postulate, although some of them are not Hammond-like processes as can be seen from the type assignment. β' and β_{BT} present almost identical numerical values, although the later is a drastic approximation to β' . This is, in general, a consequence of the range of validity of β_{BT} in the parameter space. Although it will not be discussed here, it is worth mentioning that chemical reactions, within the range studied in this article, span a very narrow subspace of the parameter space, which coincides with the also narrow subspace of validity of the BT approximation.¹⁹

It is noteworthy that β_{BT} successfully estimates all of the rotational barriers to be *late* or *early* according to the Hammond or anti-Hammond character of the processes, except in the case of R8 and R14. The values in parentheses under the entry β_{BT} ,

TABLE 4: Estimated TS Positions (Brønsted Coefficients)^a

system	species	energy	active mode	ν	k	C_k	K_V	β_{BT}	$\tau(\beta_0)$	β
R18	R	0.00	ω_4	943.4	5.09					
	TS	27.40				0.23	34.1	0.94	0.96	0.90
	P	27.03	ω_4	392.7	1.1724					
R19	R	0.00	ω_1	268.2	0.06					
	TS	5.13				6.40	84.3	0.30	0.33	0.25
	P	-42.69	ω_4	750.8	0.36					
R20	R	0.00	ω_5	1230.1	1.90					
	TS	39.82				0.48	174.9	0.38	0.30	0.48
	P	-8.01	ω_4	1927.7	0.92					
R21	R	0.00	ω_3	1208.1	1.06					
	TS	39.20				1.08	216.7	0.39	0.39	0.43
	P	-32.39	ω_4	1341.3	1.15					
R22	R	0.00	ω_2	723.0	0.42					
	TS	14.53				0.43	44.5	0.51	0.55 (0.52)	0.57
	P	6.34	ω_2	521.9	0.18					
R23	R	0.00	ω_2	693.1	0.40					
	TS	15.56				0.44	49.92	0.49	0.55 (0.51)	0.56
	P	5.81	ω_2	520.6	0.18					
R24	R	0.00	ω_1	509.2	0.73					
	TS	44.84				0.88	184.3	0.47	0.59	0.49
	P	-2.48	ω_2	474.3	0.64					
R25	R	0.00	ω_1	466.1	0.59					
	TS	31.34				0.93	128.2	0.48	0.60	0.49
	P	-1.45	ω_2	431.0	0.54					
R26	R	0.00	ω_1	422.4	0.13					
	TS	8.79				0.66	32.8	0.48	0.45 (0.48)	0.52
	P	1.19	ω_1	355.6	0.09					
R27	R	0.00	ω_1	428.3	0.13					
	TS	9.98				0.71	37.5	0.48	0.46 (0.49)	0.52
	P	1.18	ω_1	374.7	0.10					

^a Energies in kcal mol⁻¹; force constants in mdyne Å⁻¹; frequencies in cm⁻¹.

which were determined from ab initio force constants with ω_1 as the active normal mode, in most cases improve the results and in particular in the case of R8 and R14. While it might appear evident that this improvement is due to the more accurate force constant ratio C_k from the ab initio calculations, part of the improvement actually comes from a better estimate of K_V when obtained from the Marcus equation.

4.2. Intramolecular Reordering Reactions: R18–R27.

Table 4 shows the energies of reactant, transition state, and products of the R18–R27 reaction set. Along with them, the normal vibrational mode that leads reactants and products into TS is shown; these normal modes have frequency ν and force constants k . As outlined in section 2.4, K_V arises from the Marcus equation (using calculated ΔV^\ddagger) and C_k , the ratio between the ab initio force constants. Remember that τ is an index defined through the distance matrix (eq 20), whereas β and β_{BT} arise from $V_0[\omega]$ and $V[\omega]$ potential functions, respectively. Values of β and β_{BT} should be compared with the reference τ index. For R22, R23, R26, and R27 β and β_{BT} have to be compared with the value in parentheses under the τ entry, which corresponds to β_0 , because these reactions also correspond to rotational isomerizations.

In general, there is good agreement between both β and β_{BT} and the τ index, although the β_{BT} values are in better agreement with τ specially in R18–R21. For those cases, the mean absolute deviation (MAD) of β and β_{BT} from τ is 0.09 and 0.03, respectively. Within the rotational processes (R22, R23, R26, and R27), the deviation with respect to τ is 0.04 for both β and β_{BT} . Nevertheless, when compared with the β_0 values (in parentheses), β_{BT} shows a far better agreement than β (MAD equals 0.01 and 0.04, respectively). For R24 and R25 the β

and β_{BT} are quite similar, while the τ index deviates from them in almost the same amount. Note that R24 and R25 correspond to the same proton-transfer reaction at different levels of theory.

The overall good agreement of β_{BT} with τ is indeed an interesting result, although it should be noted that comparisons should not be taken too far because of the very different nature of these two indexes.

5. Concluding Remarks

An extension of the Hammond postulate that includes structural information in the characterization of the Hammond or anti-Hammond behavior of chemical reactions was presented. It has been shown that the inclusion of the force constants associated with reactants and products through an additional structural parameter makes the difference between the HP and the EHP; the thermodynamic tendency imposed by the HP is modulated, or surpassed, by the structural characteristics of products and reactants.

It has been shown that switching from HP to EHP behaviors through adding a new term in the potential energy function strongly influences the TS position through the structural-thermodynamic index γ , which determines β_{BT} , but has little effect on the barrier height. The Marcus equation for the energy of the transition state remains, to a large extent, valid within the EHP scheme.

The theoretical development presented is strongly supported by the numerical results allowing a complete characterization of different types of chemical reactions.

Acknowledgment. This work was supported by FOND-ECYT through Project No. 1020534. F.B. is a CONICYT fellow.

References and Notes

- (1) Hammond, G. S. *J. Am. Chem. Soc.* **1955**, *77*, 334.
- (2) Farcasiu, D. *J. Chem. Educ.* **1975**, *52*, 76.
- (3) Agmon, N. *J. Chem. Soc., Faraday Trans. 2* **1978**, *74*, 388.
- (4) Leffler, J. E. *Science* **1953**, *117*, 340.
- (5) Murdoch, J. R. *J. Am. Chem. Soc.* **1972**, *94*, 4410.
- (6) Miller, A. R. *J. Am. Chem. Soc.* **1978**, *100*, 1984.
- (7) Cioslowski, J. *J. Am. Chem. Soc.* **1991**, *113*, 6756.
- (8) See, for example: Carbó-Dorca, R.; Besalú, E. *J. Mol. Struct. (THEOCHEM)* **1998**, *451*, 11 and references therein.
- (9) Arteca, G. A.; Mezey, P. G. *J. Phys. Chem.* **1989**, *93*, 4746.
- (10) Arteca, G. A.; Mezey, P. G. *J. Comput. Chem.* **1988**, *9*, 728.
- (11) Cárdenas-Lailhacar, C.; Zerner, M. C. *Int. J. Quantum Chem.* **1999**, *75*, 563.
- (12) Toro-Labbé, A. *J. Mol. Struct. (THEOCHEM)* **1988**, *180*, 209.
- (13) Toro-Labbé, A. *J. Mol. Struct. (THEOCHEM)* **1990**, *207*, 247.
- (14) Bock, C. W.; Toro-Labbé, A. *J. Mol. Struct. (THEOCHEM)* **1991**, *232*, 239.
- (15) Cárdenas-Jirón, G. I.; Toro-Labbé, A.; Bock, C. W.; Maruani, J. In *Structure and Dynamics of Non-Rigid Molecular Systems*; Smeyers, Y. G., Ed.; Kluwer Academic: Dordrecht, The Netherlands, 1995; p 97.
- (16) Cárdenas-Jirón, G. I.; Gutiérrez-Oliva, S.; Melin, J.; Toro-Labbé, A. *J. Phys. Chem. A* **1997**, *101*, 4621. Cárdenas-Jirón, G. I.; Letelier, J. R.; Toro-Labbé, A. *J. Phys. Chem. A* **1998**, *102*, 7864. Gutiérrez-Oliva, S.; Letelier, J. R.; Toro-Labbé, A. *Mol. Phys.* **1999**, *96*, 61. Jaque, P.; Toro-Labbé, A. *J. Phys. Chem. A* **2000**, *104*, 995. Pérez, P.; Toro-Labbé, A. *J. Phys. Chem. A* **2000**, *104*, 1557.
- (17) Toro-Labbé, A. *J. Phys. Chem. A* **1999**, *103*, 4398.
- (18) Marcus, R. A. *Annu. Rev. Phys. Chem.* **1964**, *15*, 155.
- (19) Margalef-Roig, J.; Miret-Artés, S.; Toro-Labbé, A. *J. Phys. Chem. A* **2000**, *104*, 11589.
- (20) Frisch, M. J.; Trucks, G. W.; Schlegel, H. B.; Scuseria, G. E.; Robb, M. A.; Cheeseman, J. R.; Zakrzewski, V. G.; Montgomery, J. A., Jr.; Stratmann, R. E.; Burant, J. C.; Dapprich, S.; Millam, J. M.; Daniels, A. D.; Kudin, K. N.; Strain, M. C.; Farkas, O.; Tomasi, J.; Barone, V.; Cossi, M.; Cammi, R.; Mennucci, B.; Pomelli, C.; Adamo, C.; Clifford, S.; Ochterski, J.; Petersson, G. A.; Ayala, P. Y.; Cui, Q.; Morokuma, K.; Malick, D. K.; Rabuck, A. D.; Raghavachari, K.; Foresman, J. B.; Cioslowski, J.; Ortiz, J. V.; Stefanov, B. B.; Liu, G.; Liashenko, A.; Piskorz, P.; Komaromi, I.; Gomperts, R.; Martin, R. L.; Fox, D. J.; Keith, T.; Al-Laham, M. A.; Peng, C. Y.; Nanayakkara, A.; Gonzalez, C.; Challacombe, M.; Gill, P. M. W.; Johnson, B. G.; Chen, W.; Wong, M. W.; Andres, J. L.; Head-Gordon, M.; Replogle, E. S.; Pople, J. A. *Gaussian 98*, revision A.7; Gaussian, Inc.: Pittsburgh, PA, 1998.
- (21) Bulat, F.; Toro-Labbé, A. *Chem. Phys. Lett.* **2002**, *354*, 508.
- (22) Gonzales, J. M.; Cox, R. S., III; Brown, S. T.; Allen, W. D.; Schaefer, H. F., III *J. Phys. Chem. A* **2001**, *105*, 11327.
- (23) Petersson, G. A.; Tensfeldt, T. G.; Montgomery, J. A., Jr. *J. Am. Chem. Soc.* **1992**, *114*, 6133.
- (24) Solà, M.; Toro-Labbé, A. *J. Phys. Chem. A* **1999**, *103*, 8847.
- (25) Delaere, D.; Raspoet, G.; Nguyen, M. T. *J. Phys. Chem. A* **1999**, *103*, 171.